Colloids and Surfaces B: Biointerfaces 186 (2020) 110683

Contents lists available at ScienceDirect

Colloids and Surfaces B: Biointerfaces

journal homepage: www.elsevier.com/locate/colsurfb

A laccase based biosensor on AuNPs-MoS_2 modified glassy carbon electrode for catechol detection

Yanan Zhang[a], Xin Li[a], Dawei Li[a], Qufu Wei[a,b,*]

[a] Key Laboratory of Eco-Textiles, Ministry of Education, Jiangnan University, 1800 Lihu Avenue, Jiangsu Province, Wuxi 214122, PR China
[b] Fujian Key Laboratory of Novel Functional Textile Fiber and Materials, Minjiang University, Fuzhou, Fujian, 350108, PR China

ARTICLE INFO

Keywords:
Biosensor
MoS_2 nanosheets
Gold nanoparticles
Laccase
Catechol detection

ABSTRACT

As a kind of two-dimensional layered nanomaterial, MoS_2 nanosheets have been widely used in the field of biosensors. In this work, a novel laccase based biosensor for catechol detection was fabricated based on a nanocomposite of MoS_2 nanosheets and gold nanoparticles. The experimental results demonstrated that MoS_2 had large specific surface area and good biocompatibility, which provided abundant position for enzyme immobilization. Gold nanoparticles enhanced conductivity of MoS_2 and improved detection sensitivity. Because of the synergistic effect of MoS_2 nanosheets and gold nanoparticles, the laccase based bioelectrode exhibited a linear response to catechol from 2 to 2000 μM with a detection limit of 2 μM (S/N = 3), as well as good selectivity, stability, repeatability, and reproducibility.

1. Introduction

Most phenols are toxic and difficult to degrade, which in the environment are mainly originated from pesticide, dyes and pharmaceuticals [1,2]. As one of the phenol compounds, catechol possesses serious harm to plants, animals, and human health [3,4]. Thus, it is significant to develop a facile and low-cost method for catechol detection. Currently, enzyme based biosensors have received great attention because of their advantages, such as fast response, high sensitivity, easy operation, and continuous on-line detection [3,5]. Laccase (Lac) is phenol oxidases in the family of multi-copper oxidases, which is widely distributed in plants, insects, and fungi [6]. Lac is usually used in waste detoxification, textile dye conversion, food industry, biosensors, and analytical applications [7–13]. The oxidative reaction between Lac and phenolic substrates leads to the oxidization of phenolic hydroxyl and the reduction of O_2 to water, which could generate electrical signal [12,14].

Selection of a suitable electrocatalyst is essential to enhancing the sensing performance of electrochemical biosensors. To improve the electron transfer efficiency between the redox-active site and electrode, a variety of nanomaterials forenzyme immobilization were developed. Metals, semiconductors, magnetic materials and carbon-based materials have been widely used in enzyme immobilization [1,15–18]. Due to easy aggregation and poor processability, the main challenge of this materials is still difficult to assemble into the sensing platform [19,20]. Two-dimensional (2D) layered nanomaterials such as graphene and transition metal dichalcogenides (TMDs) have been widely employed as biosensor support materials due to their unique physical and chemical properties [21–24]. As a kind of TDMs, MoS_2 has many excellent properties for enzyme immobilization such as high specific surface area, good biocompatibility, structural stability, and large junction area with electrode/reactants [25]. In recent years, MoS_2 and its hybrids have been widely employed in the field of sensors [26–29].

Unlike carbon materials which have excellent conductivity, MoS_2 (2 H) is a semiconductor. Compared with the zero-bandgap of graphene, the bandgap of MoS_2 (2 H) could change from 1.2 to 1.9 eV depending on the number of layers [30]. To solve the problem of poor conductivity of MoS_2, it would be an ideal strategy to use the conjugation of MoS_2 nanostructures with highly conductive additives such as carbon materials, noble metals, transition metals, and polymers [31–34]. The strategy of combining two or more different materials to produce composite materials can minimize the disadvantages and maximize the advantages of a single component. For instance, Vasilescu et al. [31] have immobilized Lac on MoS_2 modified by graphene quantum dots and obtained an admirable biosensor for the detection of catechol. Owing to their high specific surface area, excellent conductivity, high chemical stability, greater biocompatibility and catalytic activity, gold nanoparticles (AuNPs) are able to significantly improve

* Corresponding author at: Key Laboratory of Eco-Textiles, Ministry of Education, Jiangnan University, 1800 Lihu Avenue, Jiangsu Province, Wuxi 214122, PR China.
E-mail address: qfwei@jiangnan.edu.cn (Q. Wei).

https://doi.org/10.1016/j.colsurfb.2019.110683
Received 29 September 2019; Received in revised form 24 November 2019; Accepted 27 November 2019
Available online 28 November 2019
0927-7765/

the performance of sensors [35–38]. AuNPs could not only enhance the conductivity of MoS_2, but also increase the surface area of MoS_2 nanosheets.

The enzyme immobilized on the surface without protection or chemical bonding is easily detached and contaminated by the environment, which affects the stability and reusability of the biosensor [39]. As a powerful electrochemical binder, Nafion has excellent proton conductivity, film formation and biocompatibility. which is effective in immobilizing a variety of enzymes [40–45]. In this work, MoS_2 nanosheets and AuNPs were prepared by simple hydrothermal and chemical reduction methods respectively. Then, MoS_2 nanosheets and AuNPs were self-assembled stably by electrostatic attraction. Further more, the Lac and AuNPs-MoS_2 mixture were fixed on the glassy carbon electrode (GCE) surface by Nafion. Following the modification of MoS_2-AuNPs, the Lac based biosensor (MoS_2-AuNPs-Lac/GCE) was successfully prepared and demonstrated good detection performance for catechol.

2. Experiments

2.1. Reagents

Thiourea, $(NH_4)_6Mo_7O_{24}{\cdot}2H_2O$, trisodium citrate dehydrate, CH_3COONa, CH_3COOH, $K_3[Fe(CN)_6]$, $K_4[Fe(CN)_6]{\cdot}3H_2O$, KCl, resorcinol, salicylic acid, phenol were purchased from Sinopharm Chemical Reagent Co., Ltd. (Shanghai, China). Lac (activity ≧50 units/mg), catechol, and p-nitrophenol were obtained from Sigma Aldrich Chemical Co., Ltd. (St. Louis, MO, USA). $HAuCl_4{\cdot}H_2O$ and Nafion (5 % w/w) were supplied by Shanghai Vita Chemical Reagent Co., Ltd and E. I. DuPont Company, respectively. 0.2 M acetate buffer solution was prepared by mixing solutions of CH_3COOH and CH_3COONa. All reagents in this work were of analytical grade without further purification. All aqueous solutions were prepared with deionized water.

2.2. Instrumentation

The morphologies of AuNPs-MoS_2 were observed through JEOL/JEM-2100 (Japan) transmission electron microscope (TEM) with a working voltage of 200 kV. The crystalline structure was analyzed by a Powder D8 Advance X-ray diffraction (XRD, Bruker AXS D8) with Cu-Ka radiation (0.15418 nm). Electrochemical experiments were carried out on a CHI 660E electrochemical workstation (CH Instruments, Shanghai, China). A saturated calomel electrode (SCE), a Pt wire, and a glassy carbon electrode (GCE with diameter of 3 mm and an area of 0.071 cm^2) were used as the reference electrode, counter electrode and working electrode, respectively.

2.3. Preparation of AuNPs-MoS_2

MoS_2 was hydrothermally obtained [46]. 1.0 mM $(NH_4)_6Mo_7O_{24}{\cdot}2H_2O$ and 30 mM thiourea were formulated into a 30 mL aqueous solution. The solution was transferred to a Teflon-lined stainless-steel autoclave and heated at 200 ℃ for 20 h. The black product was washed multiple times by deionized water and ethanol and dried in a vacuum oven at 60 ℃ for the next step.

AuNPs was prepared by chemical reduction [47]. Prior to reaction, all glassware were washed by aqua regia (HCl/HNO_3 = 3:1 Vol). 17.9 mg $HAuCl_4{\cdot}H_2O$ was dissolved in 50 ml deionized water and heated to boiling after which 5.4 mL 38.8 mM sodium citrate aqueous solution was added. The solution was stirred slowly until its color turned into wine red (AuNPs sol). 50 mg MoS_2 was then mixed with AuNPs sol and incubated at room temperature for 3 h. The resulting suspension was rewashed several times with deionized water and ethanol to remove unassembled AuNPs and other impurities. Finally, the AuNPs-MoS_2 was obtained after centrifugation and vacuum drying.

2.4. Fabrication of MoS_2-AuNPs-Lac/GCE biosensor

Prior to use, GCE was carefully polished with alumina slurry to produce a mirror-like surface. Then, GCE was sonicated in ethanol and deionized water, respectively, and the electrode was dried under natural conditions. 12 mg Lac and 16 mg AuNPs-MoS_2 were dispersed into 4 mL acetate buffer solution (0.1 M pH: 5) after which 60 μL Nafion was dropped into the suspension and was sonicated in ice-bath for 30 min to get a metastable dispersion. 5 μL of the suspension was dropped onto the GCE surface and dried at 4 ℃ overnight. The biosensor was fabricated through the above steps and named as AuNPs-MoS_2-Lac/GCE. For comparison, Lac/GCE and MoS_2-Lac/GCE biosensors were prepared without AuNPs-MoS_2 and AuNPs, respectively. MoS_2/GCE and AuNPs-MoS_2/GCE were also prepared without Lac and Nafion for Electrochemical impedance spectroscopy (EIS) experiments.

3. Results and discussion

3.1. Characterizations

The preparation process and structure of AuNPs-MoS_2-Lac/GCE biosensor are shown in Fig. 1. To determine the phase composition

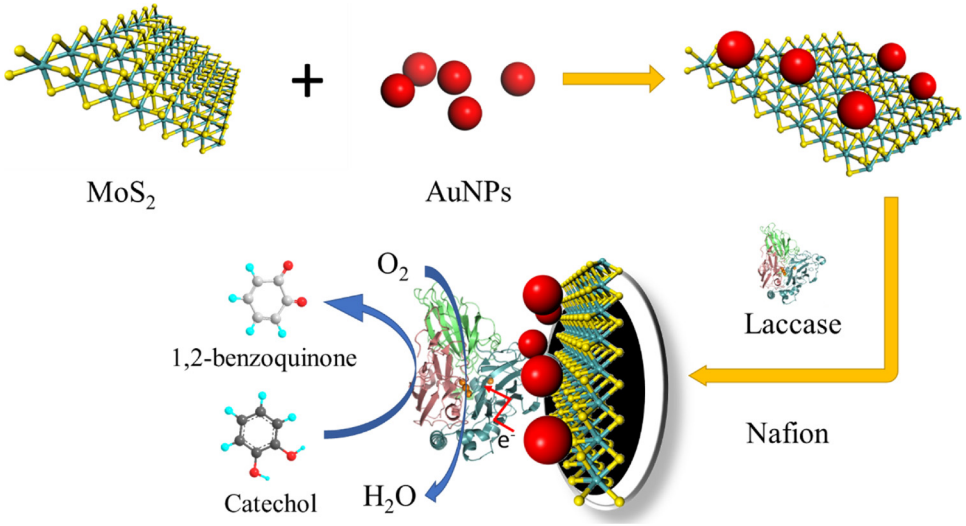

Fig. 1. Schematic illustration of the fabrication of AuNPs-MoS_2-Lac/GCE and catalyzed oxidation of catechol on the electrode surface.

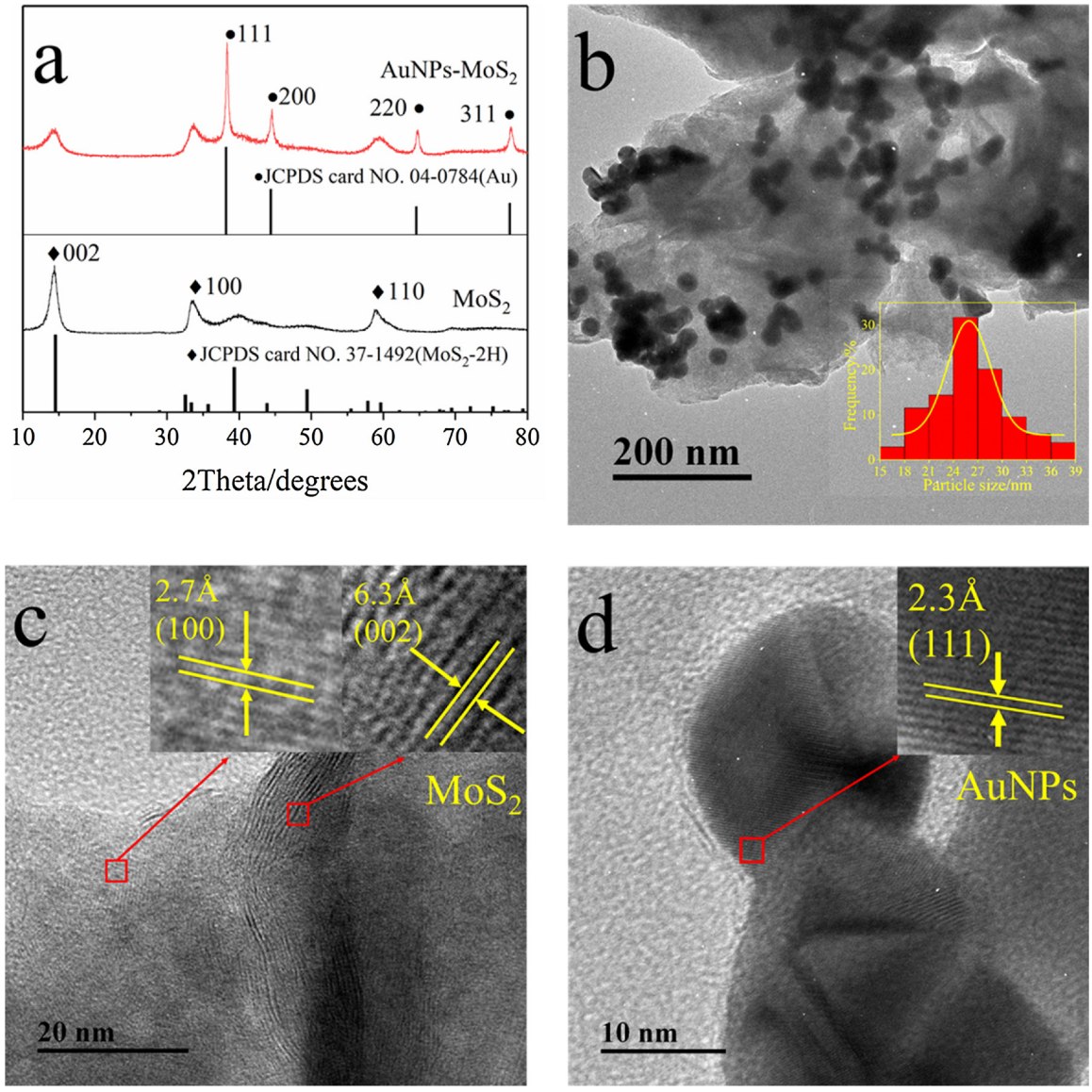

Fig. 2. (a) XRD patterns, (b) TEM and (c, d) HR-TEM imagines of AuNPs-MoS_2. Inset in b shows the particle size distribution of AuNPs.

structure of the MoS_2 and AuNPs-MoS_2, XRD analysis was conducted. As shown in Fig. 2a, three XRD peaks of pure MoS_2 at 14°, 33.5°, 58.9° are indexed to (002), (100), (110) planes of the pristine 2H-MoS_2 (JCPDS Card NO. 37-1492).Compared with MoS_2, Four new peaks of AuNP-MoS_2 emerge at 38.2°, 44.4°, 64.5°and 77.6° which are indexed to (111), (200), (220) and (311) planes of the Au (JCPDS Card NO. 04-0784), respectively.

The morphologies of MoS_2 and AuNPs-MoS_2 were characterized using TEM and HR-TEM(High Resolution Transmission Electron Microscope). As displayed in Figs. 2b and S1a (supplementary material), MoS_2 nanosheets showed wrinkled and folded sheet morphologies and agglomerated into irregular spheres with a diameter of about 500 nm. Fig. 2c shows that the MoS_2 nanosheets consisted of 15–25 single layers, and the layer-to-layer spacing was approximately 6.3 Å, which was confirmed by XRD pattern (002). It was known that the lamellar structure of MoS_2 could offer a large number of immobilization positions and reaction sites for Lac and AuNPs [12]. As revealed in Figs. 2b and S1b, all AuNPs were distributed on the MoS_2 surface without massive aggregation, which indicated a good affinity between MoS_2 nanosheets and AuNPs. Inset imagine of Fig. 2b reveals that AuNPs had diameters between 15 nm and 40 nm with an average of 26 nm. The AuNPs prepared had smaller diameters, which meant they had a larger specific surface area and better electrocatalytic performance. More detailed information was provided by HR-TEM image of AuNPs (Fig. 2d), in which clear lattice fringes were observed with the interplanar distance of 2.3 Å corresponding to the (111) crystal planes.

EIS experiments were conducted to characterize the charge transfer properties of bare electrode and electrodes modified by MoS_2 and AuNPs-MoS_2. The electrodes were tested in 5 mM $[Fe(CN)_6]^{3-/4-}$ solution containing 0.1 M KCl. In Nyquist plots (Fig. 3a), it could be seen that all curves consisted of a semicircle and a straight line, which indicated both limited electron transfer and diffusion process occurred simultaneously. According to the fitting results, the electron transfer resistances (Rct) of GCE, MoS_2/GCE, and AuNPs-MoS_2/GCE were 445 Ω, 569 Ω, and 345 Ω, respectively. Compared with bare GCE, the Rct value of MoS_2 was increased, which was due to the semiconductor property of MoS_2 (2 H). After AuNPs were assembled on MoS_2 surface, Rct value was significantly decreased and lower than that of GCE. It was reported that the work function caused by Fermi energy difference between noble metals and semiconductor materials can effectively promote electron transfer [48,49]. The $AuNP_S$ on the surface of MoS_2 can act as additional e-resource for raising fermi energy even higher [50]. The lower Rct value of AuNPs-MoS_2 was contributed to excellent conductivity and higher Fermi level of AuNPs, which promoted the

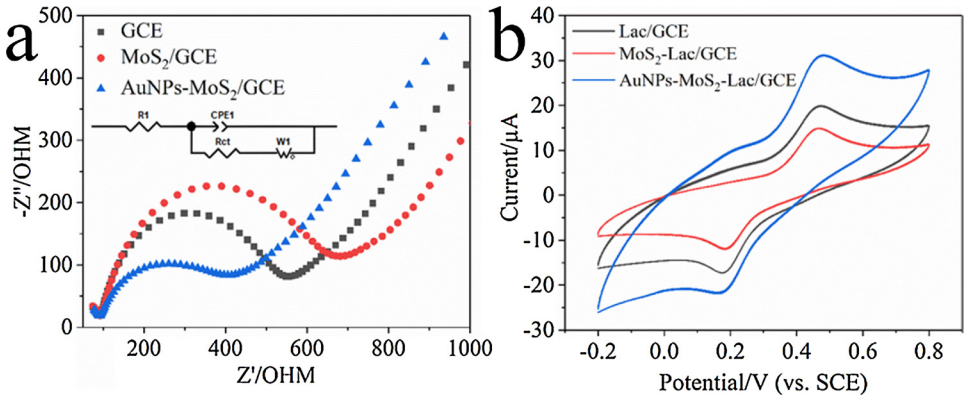

Fig. 3. (a) EIS behaviors of bare GCE, MoS_2/GCE and AuNPs-MoS_2/GCE in 5 mM $[Fe(CN)_6]^{3-/4-}$ solution containing 0.1 M KCl. (b) CVs of Lac/GCE, MoS_2-Lac/GCE and AuNPs-MoS_2-Lac/GCE in 0.2 M acetate buffer solution (pH 5.0) containing 350 μM catechol.

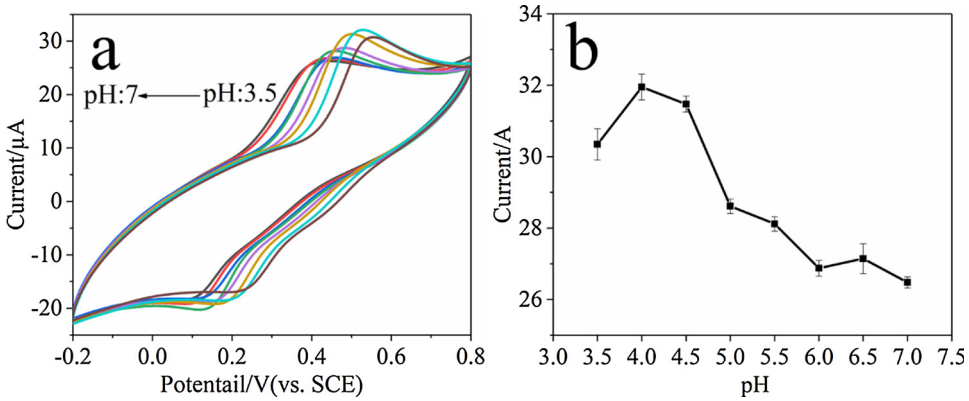

Fig. 4. (a) CVs of AuNPs-MoS_2-Lac/GCE in 0.2 M acetate buffer solution containing 350 μM catechol in the pH of 3.5, 4.0, 4.5, 5.0, 5.5, 6.0, 6.5 and 7.0. (b) The plot of the oxidation peak current against the pH.

electron transfer between MoS_2 and redox species. The presence of AuNPs significantly reduced the electrical impedance of MoS_2 and improved the electron transfer efficiency, which facilitates the sensitivity and application potential of MoS_2 based biosensors.

3.2. Electrochemical behaviors of the fabricated biosensors

Fig. 3b shows the CVs of different enzyme electrodes in acetate buffer solution (0.2 M, pH 5.0) with 350 μM of catechol. The catalyzed reaction mechanism illustrated in Fig. 1 is described as follows [15].

$$\text{Catechol} + \text{Laccase(oxy)} \rightarrow 1,\ 2\ \text{Benzoquinone} + \text{Laccase(deoxy)} + 2H^+ + 2e \quad (1)$$

$$\text{Laccase(deoxy)} + O_2 + 4H^+ \rightarrow \text{Laccase(oxy)} + 2H_2O \quad (2)$$

It was also revealed that each of the three curves had an oxidation peak and a reduction peak, and they were all at the same potential. Compared to electrodes modified directly by Lac (Lac/GCE), the value of oxidation peak of the enzyme electrode immobilized on MoS_2 nanosheets (MoS_2-Lac/GCE) was decreased which could to an extent be attributed to the MoS_2 nanosheets impeding the transfer of electrons. It is noticeable that biosensor based on AuNPs-MoS_2 (AuNPs-MoS_2-Lac/GCE) displayed higher oxidation current peak than Lac/GCE and MoS_2-Lac/GCE. Due to the characteristics of large surface area, excellent electrocatalysis, high conductivity and vigorous adsorption ability, AuNPs promoted the electron transfer between redox species and MoS_2 and enhanced the response signals of the modified electrode [51].

In order to study the kinetics of electrode reactions, the CVs of AuNPs-MoS_2-Lac/GCE were recorded in acetate buffer solution (0.2 M pH 5.0) containing 350 μM catechol at different scan rates of $50-300\ mV\ s^{-1}$(Fig. S2). The oxidation and reduction peak currents were enhanced as the scan rates increased and were proportional to the square roots of scan rates. According to the fitting results shown in Fig. 5b, the linear regression equation is expressed as $Ipa = 6.72v^{1/2} + 2.45$ ($R^2 = 0.994$) and $Ipc = -4.25v^{1/2} - 1.70$($R^2 = 0.984$). Ipa, Ipc, and v represent the anodic peak currents (μA), cathodic peak currents (μA), and scan rates ($mV\ s^{-1}$), respectively. The result revealed that the electrochemical reaction at AuNPs-MoS_2-Lac/GCE was a typical diffusion-controlled electron-transfer process. Besides, as the scan rate increased, the anodic peak moved to a more positive potential and the cathodic peak moved to a more negative potential, which indicated a quasi-reversible electrochemical reaction process.

3.3. Optimization of AuNPs-MoS_2-Lac/GCE biosensor

To ensure the optimal performance of AuNPs-MoS_2-Lac/GCE in determination to catechol. The pH influence was investigated through the voltammetric behavior of AuNPs-MoS_2-Lac/GCE toward 350 μM catechol in the pH range between 3.5 and 7.0. As shown in Fig. 4 a and b, the oxidation currents of AuNPs-MoS_2-Lac/GCE increased with the increase of pH range from 3.5 to 4.0 and reached the maximum at pH 4.0. Further increasing the pH values resulted in the decrease in the oxidation currents. Therefore, pH 4.0 was chosen as the optimal pH value for subsequent measurements in 0.2 M acetate buffer solution

3.4. DPV responses of AuNP-MoS_2-Lac-GCE towards catechol

The DPV (differential pulse voltammetry) curves to determine catechol at different concentrations from 2 μM to 2000 μM by the AuNPs-MoS_2-Lac/GCE biosensors were obtained in acetate buffer (0.2 M pH

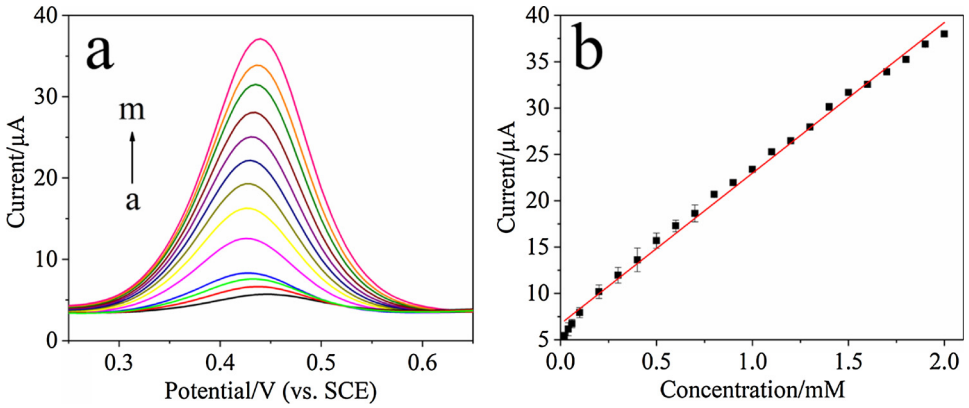

Fig. 5. (a) DPVs of catechol at AuNPs-MoS_2-Lac/GCE biosensor in 0.2 M acetate buffer solution (pH 4.0). Catechol concentration: 20, 40, 60, 100, 300, 500, 700,900,1100,1300,1500,1700 and 1900 μM (from a to m). (b) The calibration curve of DPV peaks against concentration of catechol.

4.0). As shown in Figs. 5a and S3, DPV curve had no obvious peak when there was no catechol present. It is noticeable that the electrocatalytic current increased proportionally with increasing concentration of catechol in the wide range from 2 μM to 2000 μM. Fig. 5b shows the linear calibration curve of DPV peaks against the concentration of catechol. The linear regression equation was $I = 6.708 + 16.2634C$, with a correlation coefficient of 0.9946, a sensitivity of 16.3 μA/mM and a detection limit of 2 μM (S/N = 3). I and C represent the peak currents of DPVs (μA) and concentration of catechol (mM), respectively.

Table. 1 compares the determination performance of several Lac-based electrodes toward catechol. It was observed that AuNP-MoS_2-Lac/GCE biosensor in this work showed a relatively low detection limit and a wide linear range. The broad linear range was hypothesized be due to the fact that MoS_2 nanosheets provided a large number of immobilization sites for Lac, hence promoting the reaction between the enzyme and the substrate. It was also suggested that the low detection limit was a result of the excellent conductivity and electrocatalytic properties of AuNPs. The biosensors exhibited promising performance due to the synergistic catalytic effect of MoS_2 nanosheets and AuNPs, which indicated that the hybrid structure of AuNPs-MoS_2 is beneficial to enhance the detection performance of biosensors.

3.5. Selectivity, stability and reproducibility of the biosensor

The selectivity and anti-interference ability of the biosensor was investigated by the amperometric response of AuNPs-MoS_2-Lac/GCE towards catechol and other similar chemicals structures. At potential of 0.45 V, Catechol (100 μM), resorcinol (100 μM), salicylic acid (100 μM), phenol (100 μM) and p-nitrophenol (100 μM) were sequentially added to the acetate buffer solution (0.2 M pH 4.0) under stirring. As shown in Fig. 6, AuNPs-MoS_2-Lac/GCE biosensor displayed rapid and sensitive responses to the addition of catechol. There were no significant amperometric responses observed with the addition of the interfering reagents. Upon the addition of catechol again, the biosensor still provided a strong and fast current response. The results therefore indicated that the prepared biosensor had good selectivity and anti-interference.

To investigate the repeatability and reproducibility of the biosensors, repeated experiments were carried out. A AuNPs-MoS_2-Lac/GCE biosensor was tested successively for 10 times in solution containing 1 mM catechol. As shown in Fig. S4, The DPV peak of the tenth test was only 3 % lower than the initial value and the relative standard deviation (RSD) of the peak values of DPVs was 1.2 %, which indicated good reusability of the biosensor. Five biosensors were prepared and tested under the same condition. The RSD of the peak values of DPVs current was 0.7 %, indicating that the biosensor possessed excellent reproducibility. The test of stability of the biosensor was also carried out in air at 4 °C. As shown in Fig. S5, the peak value of DPV current was deceased by only 5 % after half a month later. Even after a month, the biosensor still retained 90 % of the initial value, which attributed to the biocompatibility of AuNPs-MoS_2 and Nafion. This results suggested that this novel sensor had application value for detecting catechol.

Table 1
Performance comparison of different Lac based electrodes toward catechol.

electrode description	detection limit (μM)	linear range (μM)	reference
Lac/AP-rGOs/Chit/GCE	7	15–700	[52]
FYSSns–2–Lac/GCE	1.6	12.5–450	[3]
Lac-a-Fe_2O_3NC-CPE	4.28	8-800	[53]
Lac–Nafion–ECNFs/GCE	0.63	1–1300	[54]
AuNP-MoS_2-Lac/GCE	2	2–2000	This work

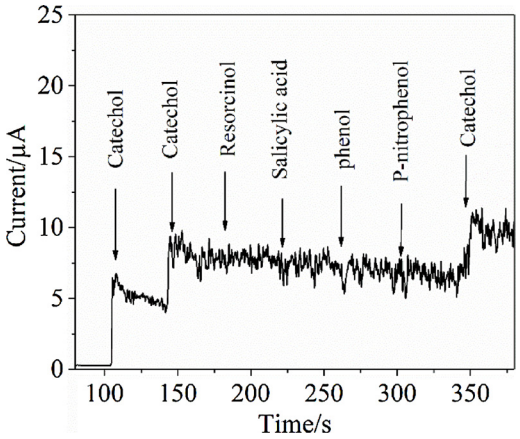

Fig. 6. Amperometric responses of AuNPs-MoS_2-Lac/GCE after the addition of 100 μM catechol and different interfering substances in 0.2 M acetate buffer solution (pH 4.0) at 0.45 V.

4. Conclusion

In conclusion, a Lac biosensor based on AuNPs-MoS_2 had been prepared and characterized. The results shown that the nanocomposite of AuNPs-MoS_2 enhanced the performance of Lac based biosensors. The as-prepared biosensor exhibited a wide linear range, low detection limit, good selectivity, stability, and reproducibility which was attributed to the large surface area, excellent biocompatibility, fast mass transport, and synergistic catalytic of AuNPs-MoS_2. The excellent performance of AuNPs-MoS_2-Lac/GCE demonstrates that it would be a promising biosensor for of catechol detection.

Author contributions section

Yanan Zhang designed the experiment, performed the experiment and wrote the manuscript.

Xin Li performed the experiment and analyzed the data.

Dawei Li analyzed the data and revised the manuscript.

Qufu Wei analyzed the data and revised the manuscript.

Declaration of Competing Interest

There are no conflicts to declare.

Acknowledgements

This research was financially supported by the national first-class discipline program of Light Industry Technology and Engineering (LITE2018-21), the Natural Science Foundation of Jiangsu Province (BK20180628), the National Science Foundation of China (51803078), 111 Project (B17021), the Fundamental Research Funds for the Central Universities (JUSRP11701), the Priority Academic Program Development of Jiangsu Higher Education Institutions, Top-notch Academic Programs Project of Jiangsu Higher Education Institutions (PPZY2015B147).

Appendix A. Supplementary data

Supplementary material related to this article can be found, in the online version, at doi:https://doi.org/10.1016/j.colsurfb.2019.110683.

References

[1] J. Yang, D. Li, J. Fu, F. Huang, Q. Wei, TiO_2-CuCNFs based laccase biosensor for enhanced electrocatalysis in hydroquinone detection, Electroanal. Chem. 766 (2016) 16–23.
[2] D. Jiang, J. Pang, Q. You, T. Liu, Z. Chu, W. Jin, Simultaneous biosensing of catechol and hydroquinone via a truncated cube-shaped Au/PBA nanocomposite, Biosens. Bioelectron. 124 (2019) 260–267.
[3] Y. Zheng, D. Wang, Z. Li, X. Sun, T. Gao, G. Zhou, Laccase biosensor fabricated on flower–shaped yolk–shell SiO_2 nanospheres for catechol detection, Colloids Surf. A 538 (2018) 202–209.
[4] F. Karim, A.N.M. Fakhruddin, Recent advances in the development of biosensor for phenol: a review, Rev. Environ. Sci. Biotechnol. 11 (2012) 261–274.
[5] M. Nazari, S. Kashanian, R. Rafipour, Laccase immobilization on the electrode surface to design a biosensor for the detection of phenolic compound such as catechol, Spectrochim. Acta A. Mol. Biomol. Spectrosc. 145 (2015) 130–138.
[6] V. Madhavi, S.J.B. Lele, Laccase: properties and applications, Bioresources 4 (2009) 1694–1717.
[7] P. Lv, H. Zhou, A. Mensah, Q. Feng, D. Wang, X. Hu, Y. Cai, L. Amerigo Lucia, D. Li, Q. Wei, A highly flexible self-powered biosensor for glucose detection by epitaxial deposition of gold nanoparticles on conductive bacterial cellulose, Chem. Eng. J. 351 (2018) 177–188.
[8] R. Chandra, P.J.E.S.P. Chowdhary, Impacts, properties of bacterial laccases and their application in bioremediation of industrial wastes, Environ. Sci.-proc. Imp. 17 (2015) 326–342.
[9] J.F. Osma, J.L. Toca-Herrera, S.J.Er. Rodríguez-Couto, Uses of laccases in the food industry, Enzyme Res. 2010 (2010).
[10] E. Abadulla, T. Tzanov, S. Costa, K.-H. Robra, A. Cavaco-Paulo, G.M.J.A.E.M. Gübitz, Decolorization and detoxification of textile dyes with a laccase from Trametes hirsuta, Appl. Environ. Microbiol. 66 (2000) 3357–3362.
[11] M.Y. Arıca, B. Altıntas, G.J.Bt. Bayramoğlu, Immobilization of laccase onto spacer-arm attached non-porous poly (GMA/EGDMA) beads: application for textile dye degradation, Bioresour. Technol. Rep. 100 (2009) 665–669.
[12] S.A.R. Albayati, S. Kashanian, M. Nazari, S.J.B.o.M.S. Rezaei, Novel fabrication of a laccase biosensor to detect phenolic compounds using a carboxylated multiwalled carbon nanotube on the electropolymerized support, Bull. Mater. Sci. 42 (2019) 187.
[13] X. Li, P. Lv, Y. Yao, Q. Feng, A. Mensah, D. Li, Q. Wei, A novel single-enzymatic biofuel cell based on highly flexible conductive bacterial cellulose electrode utilizing pollutants as fuel, Chem. Eng. J. 379 (2020) 122316.
[14] M.M. Rodríguez-Delgado, G.S. Alemán-Nava, J.M. Rodríguez-Delgado, G. Dieck-Assad, S.O. Martínez-Chapa, D. Barceló, R. Parra, Laccase-based biosensors for detection of phenolic compounds, Trac-trend. Anal. Chem. 74 (2015) 21–45.
[15] L.P. Mei, J.J. Feng, L. Wu, J.Y. Zhou, J.R. Chen, A.J. Wang, Novel phenol biosensor based on laccase immobilized on reduced graphene oxide supported palladium-copper alloyed nanocages, Biosens. Bioelectron. 74 (2015) 347–352.
[16] J. Fu, H. Qiao, D. Li, L. Luo, K. Chen, Q. Wei, Laccase biosensor based on electrospun copper/carbon composite nanofibers for catechol detection, Sensors (Basel) 14 (2014) 3543–3556.
[17] S. Palanisamy, S.K. Ramaraj, S.M. Chen, T.C. Yang, P. Yi-Fan, T.W. Chen, V. Velusamy, S. Selvam, A novel laccase biosensor based on laccase immobilized graphene-cellulose microfiber composite modified screen-printed carbon electrode for sensitive determination of catechol, Sci. Rep. 7 (2017) 41214.
[18] A. Boujakhrout, S. Jimenez-Falcao, P. Martinez-Ruiz, A. Sanchez, P. Diez, J.M. Pingarron, R. Villalonga, Novel reduced graphene oxide-glycol chitosan nanohybrid for the assembly of an amperometric enzyme biosensor for phenols, Analyst 141 (2016) 4162–4169.
[19] D. Li, M.B. Müller, S. Gilje, R.B. Kaner, G.G.J.N.n. Wallace, Processable aqueous dispersions of graphene nanosheets, Nat. Nanotechnol. 3 (2008) 101.
[20] B.G. Choi, J. Im, H.S. Kim, H.J.E.A. Park, Flow-injection amperometric glucose biosensors based on graphene/Nafion hybrid electrodes, Electrochim. Acta 56 (2011) 9721–9726.
[21] G. Alarcon-Angeles, M. Palomar-Pardavé, A. Merkoçi, 2D materials-based platforms for electroanalysis applications, Electroanal 30 (2018) 1271–1280.
[22] T. Kuila, S. Bose, P. Khanra, A.K. Mishra, N.H. Kim, J.H. Lee, Recent advances in graphene-based biosensors, Biosens. Bioelectron. 26 (2011) 4637–4648.
[23] A. Sinha, B. Dhanjai, Y. Tan, H. Huang, X. Zhao, J. Dang, R.Jain Chen, MoS_2 nanostructures for electrochemical sensing of multidisciplinary targets: a review, Trac-trend. Anal. Chem. 102 (2018) 75–90.
[24] G. Maduraiveeran, M. Sasidharan, V. Ganesan, Electrochemical sensor and biosensor platforms based on advanced nanomaterials for biological and biomedical applications, Biosens. Bioelectron. 103 (2018) 113–129.
[25] X. Gan, H. Zhao, X. Quan, Two-dimensional MoS_2: a promising building block for biosensors, Biosens. Bioelectron. 89 (2017) 56–71.
[26] P.K. Pathania, J.K. Saini, S. Vij, R. Tewari, P. Sabherwal, P. Rishi, C.R. Suri, Aptamer functionalized MoS_2-rGO nanocomposite based biosensor for the detection of Vi antigen, Biosens. Bioelectron. 122 (2018) 121–126.
[27] P.P. Li, X.P. Liu, C.J. Mao, B.K. Jin, J.J. Zhu, Photoelectrochemical DNA biosensor based on g-C_3N_4/MoS_2 2D/2D heterojunction electrode matrix and co-sensitization amplification with CdSe QDs for the sensitive detection of ssDNA, Anal. Chim. Acta 1048 (2019) 42–49.
[28] S. Wang, S. Zhang, M. Liu, H. Song, J. Gao, Y. Qian, MoS_2 as connector inspired high electrocatalytic performance of $NiCo_2O_4$ nanoplates towards glucose, Sens. Actuators B-Chem. 254 (2018) 1101–1109.
[29] L. Fang, F. Wang, Z. Chen, Y. Qiu, T. Zhai, M. Hu, C. Zhang, K. Huang, Flower-like MoS_2 decorated with Cu_2O nanoparticles for non-enzymatic amperometric sensing of glucose, Talanta 167 (2017) 593–599.
[30] A. Kuc, N. Zibouche, T. Heine, Influence of quantum confinement on the electronic structure of the transition metal sulfideTS_2, Phys. Rev. B 83 (2011).
[31] I. Vasilescu, S.A. Eremia, M. Kusko, A. Radoi, E. Vasile, G.L. Radu, Molybdenum disulphide and graphene quantum dots as electrode modifiers for laccase biosensor, Biosens. Bioelectron. 75 (2016) 232–237.
[32] S. Wu, Z. Zeng, Q. He, Z. Wang, S.J. Wang, Y. Du, Z. Yin, X. Sun, W. Chen, H. Zhang, Electrochemically reduced single-layer MoS_2 nanosheets: characterization, properties, and sensing applications, Small 8 (2012) 2264–2270.
[33] X. Lin, Y. Ni, S. Kokot, Electrochemical cholesterol sensor based on cholesterol oxidase and MoS_2 -AuNPs modified glassy carbon electrode, Sens. Actuators B-Chem. 233 (2016) 100–106.
[34] J. Huang, Y. He, J. Jin, Y. Li, Z. Dong, R. Li, A novel glucose sensor based on MoS_2 nanosheet functionalized with Ni nanoparticles, Electrochim. Acta 136 (2014) 41–46.
[35] Y. Wang, L. Wang, H. Chen, X. Hu, S. Ma, Fabrication of highly sensitive and stable hydroxylamine electrochemical sensor based on gold nanoparticles and metal-metalloporphyrin framework modified electrode, ACS Appl. Mater. Interfaces 8 (2016) 18173–18181.
[36] Z. Chang, Y. Zhou, L. Hao, Y. Hao, X. Zhu, M. Xu, Simultaneous determination of dopamine and ascorbic acid using β-cyclodextrin/Au nanoparticles/graphene-modified electrodes, Anal. Methods-UK 9 (2017) 664–671.
[37] J. Li, Y. Wang, Y. Sun, C. Ding, Y. Lin, W. Sun, C. Luo, A novel ionic liquid functionalized graphene oxide supported gold nanoparticle composite film for sensitive electrochemical detection of dopamine, RSC Adv. 7 (2017) 2315–2322.
[38] S. Su, H. Sun, W. Cao, J. Chao, H. Peng, X. Zuo, L. Yuwen, C. Fan, L. Wang, Dual-target electrochemical biosensing based on DNA structural switching on gold nanoparticle-decorated MoS_2 nanosheets, ACS Appl. Mater. Interfaces 8 (2016) 6826–6833.
[39] N. Maleki, S. Kashanian, M. Nazari, N. Shahabadi, A novel sensitive laccase biosensor using gold nanoparticles and poly L-arginine to detect catechol in natural water, Biotechnol. Appl. Biochem. 66 (2019) 502–509.
[40] Q. Huang, Z. Lu, J.F.J.L. Rusling, Composite films of surfactants, Nafion, and proteins with electrochemical and enzyme activity, Langmuir 12 (1996) 5472–5480.
[41] J. Wang, M. Musameh, Y.J.J.o.t.A.C.S. Lin, Solubilization of carbon nanotubes by Nafion toward the preparation of amperometric biosensors, J. Am. Chem. Soc. 125 (2003) 2408–2409.
[42] S.H. Lim, J. Wei, J. Lin, Q. Li, J.J.B. KuaYou, Bioelectronics, A glucose biosensor based on electrodeposition of palladium nanoparticles and glucose oxidase onto Nafion-solubilized carbon nanotube electrode, Biosens. Bioelectron. 20 (2005) 2341–2346.
[43] Q. Zhou, L. Yang, G. Wang, Y.J.B. Yang, Bioelectronics, Acetylcholinesterase biosensor based on SnO_2 nanoparticles–carboxylic graphene–nafion modified electrode for detection of pesticides, Biosens. Bioelectron. 49 (2013) 25–31.
[44] P. Norouzi, F. Faridbod, B. Larijani, M.R.J.I.J.E.S. Ganjali, Glucose biosensor based on MWCNTs-gold nanoparticles in a nafion film on the glassy carbon electrode using flow injection FFT continuous cyclic voltammetry, Biosens. Bioelectron. 5

(2010) 1213–1224.
[45] C. Guo, H. Sun, X.J.S. Zhao, A.B. Chemical, Myoglobin within graphene oxide sheets and Nafion composite films as highly sensitive biosensor, Sens. Actuators B-chem. 164 (2012) 82–89.
[46] J. Xie, J. Zhang, S. Li, F. Grote, X. Zhang, H. Zhang, R. Wang, Y. Lei, B. Pan, Y. Xie, Controllable disorder engineering in oxygen-incorporated MoS_2 ultrathin nanosheets for efficient hydrogen evolution, J. Am. Chem. Soc. 135 (2013) 17881–17888.
[47] X. Ji, X. Song, J. Li, Y. Bai, W. Yang, X. Peng, Size control of gold nanocrystals in citrate reduction: the third role of citrate, J. Am. Chem. Soc. 129 (2007) 13939–13948.
[48] Z. Zhang, J.T. Yates Jr., Band bending in semiconductors: chemical and physical consequences at surfaces and interfaces, Chem. Rev. 112 (2012) 5520–5551.
[49] P. Peerakiatkhajohn, J.-H. Yun, H. Chen, M. Lyu, T. Butburee, L. Wang, Stable hematite nanosheet photoanodes for enhanced photoelectrochemical water splitting, Adv. Mater. 28 (2016) 6405–6410.
[50] N.R. Nirala, S. Pandey, A. Bansal, V.K. Singh, B. Mukherjee, P.S. Saxena, A. Srivastava, Different shades of cholesterol: gold nanoparticles supported on MoS_2nanoribbons for enhanced colorimetric sensing of free cholesterol, Biosens. Bioelectron. 74 (2015) 207–213.
[51] M. Nazari, S. Kashanian, N. Maleki, N.J.B.o.M.S. Shahabadi, Laccase immobilized onto graphene oxide nanosheets and electrodeposited gold–-cetyltrimethylammonium bromide complex to fabricate a novel catechol biosensor, Bull. Mater. Sci. 42 (2019) 51.
[52] X.-H. Zhou, L.-H. Liu, X. Bai, H.-C. Shi, A reduced graphene oxide based biosensor for high-sensitive detection of phenols in water samples, Sens. Actuators B-chem. 181 (2013) 661–667.
[53] C. Sarika, M.S. Shivakumar, C. Shivakumara, G. Krishnamurthy, B. Narasimha Murthy, I.C. Lekshmi, A novel amperometric catechol biosensor based on alpha-Fe_2O_3 nanocrystals-modified carbon paste electrode, Artif. Cell Nanomed. B 45 (2017) 625–634.
[54] D. Li, Z. Pang, X. Chen, L. Luo, Y. Cai, Q. Wei, A catechol biosensor based on electrospun carbon nanofibers, Beilstein J. Nanotechnol. 5 (2014) 346–354.